

## Tryptophan catabolites from microbiota ameliorate immune-mediated hepatitis through activating aryl hydrocarbon receptor of T cells

Bo Li<sup>a\*</sup>, Xueying Liang<sup>a\*</sup>, Yikang Li<sup>a\*</sup>, Rui Wang<sup>a</sup>, Yiran Wei<sup>a,b</sup>, Qiaoyan Liu<sup>a</sup>, Jun Zhang<sup>a</sup>, Qixia Wang<sup>a</sup>, Qi Miao<sup>a</sup>, Xiao Xiao<sup>a</sup>, Min Lian<sup>a</sup>, Zhi Wang<sup>c</sup>, Yufeng Zhou<sup>d,e</sup>, M. Eric Gershwin<sup>f</sup>, Zhengrui You<sup>a#</sup>, Ruqi Tang<sup>a#</sup>, and Xiong Ma<sup>b,a,g#</sup>

<sup>a</sup>NHC Key Laboratory of Digestive Diseases (Renji Hospital, Shanghai Jiaotong University School of Medicine), Division of Gastroenterology and Hepatology, State Key Laboratory for Oncogenes and Related Genes, Renji Hospital, School of Medicine, Shanghai JiaoTong University; Shanghai Institute of Digestive Disease; 145 Middle Shandong Road, Shanghai 200001, China; <sup>b</sup>Department of Gastroenterology and Hepatology, Zhongshan Hospital, Fudan University, Shanghai, China; <sup>c</sup>Guanghua School of Stomatology, Guangdong Provincial Key Laboratory of Stomatology, Stomatological Hospital, Sun Yat-Sen University, Guangzhou, China; <sup>d</sup>Institute of Pediatrics, Children's Hospital of Fudan University, Shanghai, China; <sup>e</sup>National Health Commission (NHC) Key Laboratory of Neonatal Diseases, Fudan University, Shanghai, China; <sup>f</sup>Division of Rheumatology, Department of Medicine, Allergy and Clinical Immunology, University of California at Davis, Davis, CA, USA; <sup>g</sup>Institute of Aging & Tissue Regeneration, Renji Hospital, School of Medicine, Shanghai JiaoTong University, Shanghai, China

### ABSTRACT

Intestinal dysbiosis and T cell-mediated immune attack are implicated in the pathogenesis of autoimmune hepatitis (AIH). However, the mechanisms by which microbiota-derived metabolites modulate immune homeostasis in AIH remain elusive. Here, we demonstrated that microbiota-derived indole-3-carboxaldehyde (ICA) was significantly reduced in patients with AIH. Treatment with ICA restricted the activation of effector T cells by activating AhR in T lymphocytes. Nuclear translocation of AhR induced the transcription of PI3K interacting protein 1 (Pik3ip1), which inhibited the PI3K/Akt/mTOR signaling pathway. In vivo supplementation of ICA suppressed effector T cells and mitigated the tissue damage and hepatic inflammation in two mouse models of T cell-mediated hepatitis. Importantly, T cell-specific deletion of AhR abrogated the protective effects of ICA in AIH-like mouse model. Finally, administration of *Lactobacillus reuteri* resulted in elevated level of ICA and protected mice from liver damage. Our data suggest that ICA supplementation ameliorates immune-mediated hepatitis through agonizing AhR in T cells, presenting a promising therapeutic strategy for AIH.

### ARTICLE HISTORY

Received 19 January 2025  
Revised 27 August 2025  
Accepted 2 September 2025

### KEYWORDS

Indole-3-carboxaldehyde;  
aryl hydrocarbon receptor;  
PI3K interacting protein 1;  
immune-mediated hepatitis;  
*lactobacillus reuteri*

## Introduction

Autoimmune hepatitis (AIH) is an organ-specific autoimmune disorder characterized by T cell-rich infiltrates leading to necrosis of hepatocytes and hepatic fibrosis.<sup>1,2</sup> Patients of AIH generally respond to the systemic immunosuppression comprising corticosteroids and/or azathioprine.<sup>2</sup> However, there is an unmet need for alternative therapies due to the inadequate response or intolerance to the standard therapy.

Although the etiology is incompletely understood, tissue damage in AIH is triggered by the presentation of liver autoantigens to Th0 lymphocytes, leading to subsequent cascades of pro-inflammatory immune responses.<sup>2,3</sup> The clonality of the T cell receptor found in patients with AIH supports pathogenic antigen-specific T cell responses.<sup>4,5</sup> Upon activated, CD4<sup>+</sup> and CD8<sup>+</sup> T cells proliferate and differentiate into effector cells. It has been implicated that massive release of pro-inflammatory cytokines are involved in the pathogenesis of AIH, including IL-12, IFN- $\gamma$ , tumor necrosis factor- $\alpha$  (TNF- $\alpha$ ) and IL-6.<sup>3,6</sup> The presence of IL-12 promotes expansion of IFN- $\gamma$  and IL-2-producing Th1 cells, which then aberrantly activate cytotoxic T lymphocytes.<sup>3</sup> In addition, numeric and functional defects of hepatic regulatory T cells (Tregs) in AIH

**CONTACT** Xiong Ma  [maxiongmd@hotmail.com](mailto:maxiongmd@hotmail.com); Ruqi Tang  [ruqi.tang@gmail.com](mailto:ruqi.tang@gmail.com); Zhengrui You  [youzhengrui@126.com](mailto:youzhengrui@126.com)  Renji Hospital, School of Medicine, Shanghai Jiao Tong University, Shanghai Institute of Digestive Disease, 145 Middle Shandong road, Shanghai 200001, China

\*BL, XL and YL joint first co-authorship.

#XM, RT and ZY joint last co-authorship.

 Supplemental data for this article can be accessed online at <https://doi.org/10.1080/19490976.2025.2557979>

© 2025 The Author(s). Published with license by Taylor & Francis Group, LLC.

This is an Open Access article distributed under the terms of the Creative Commons Attribution-NonCommercial License (<http://creativecommons.org/licenses/by-nc/4.0/>), which permits unrestricted non-commercial use, distribution, and reproduction in any medium, provided the original work is properly cited. The terms on which this article has been published allow the posting of the Accepted Manuscript in a repository by the author(s) or with their consent.

probably contribute to the disease relapse and persistence.<sup>7,8</sup> Therefore, current immunotherapies for AIH mainly focus on inhibiting the intrahepatic inflammatory milieu and/or restoring the Treg pool.

Emerging studies have highlighted the associations between gut dysbiosis and inflammatory liver diseases including AIH.<sup>9–13</sup> In previous study, we observed an altered microbial tryptophan metabolism in patients with AIH.<sup>10</sup> Indole derivatives, produced by commensal metabolism of tryptophan, play a pivotal role in shaping host immune defense and tolerance mainly through activating aryl hydrocarbon receptor (AhR).<sup>14,15</sup> A recent study found that in a T cell-specific Tet2 knock-out mouse model, indole derivatives produced by liver-translocated *Lactobacilli* bacteria were required to induce AIH-like pathology through agonizing AhR.<sup>16</sup> However, Vuerich et al. reported that AhR signaling in Treg and Th17 cells was aberrantly inhibited in patients with AIH, leading to impaired Treg immunosuppressive function.<sup>17</sup> Blockade of AhR repressor (AHRR), however, restored T cell response to AhR and attenuated liver damage in mouse models of AIH.<sup>18</sup> Therefore, the role that AhR plays in AIH pathogenesis is elusive. In addition, it remains unknown whether microbiota-derived indoles, as a key family of AhR agonist, are associated with the disease and how they may impact immune responses in human individuals of AIH.

Phosphoinositide-3-kinase interacting protein 1 (Pik3ip1), a transmembrane protein, has recently been identified as a negative regulator of PI3K signaling.<sup>19,20</sup> Intriguingly, Pik3ip1 is preferentially expressed in T lymphocytes. Mice deficient in Pik3ip1 exhibit enhanced anti-tumor immunity and more rapid clearance of bacterial infections,<sup>8,20,21</sup> while downregulated expression of Pik3ip1 in autoimmune disorders leads to over-activation of T lymphocytes and aggravated disease.<sup>22</sup> Therefore, we hypothesize that Pik3ip1 may also serve as an immune checkpoint for modulating autoimmune responses in AIH.

Herein, we report that microbial metabolite indole-3-carboxaldehyde (ICA) is decreased in patients with AIH. Treatment with ICA induces activation of AhR in T lymphocytes, leading to increased Pik3ip1 expression, thereby mitigating liver inflammation and tissue damage. Our data suggest that supplementation of ICA may represent a promising strategy for immunotherapy of AIH.

## Methods

### Human samples

Stool samples were freshly collected from patients with AIH ( $n = 42$ ) and healthy controls ( $n = 34$ ) and immediately frozen at  $-80^{\circ}\text{C}$ . Patients with AIH were diagnosed according to criteria established by the International Autoimmune Hepatitis Group in 2008 and have not been treated with steroids or immunosuppressant.<sup>23</sup> The clinical demographical data are included in Supplementary Table S1.

### UHPLC-MS/MS profiling of tryptophan-derived metabolites

Quantification of the indole derivatives was performed by PROFLEADER (Shanghai, China) using a UHPLC-MS/MS system. Details regarding the UHPLC-MS/MS profiling of tryptophan metabolites are provided in the Supplementary Methods.

### In vitro activation and differentiation of human T cells

Peripheral blood mononuclear cells were prepared by Ficoll (GE Healthcare, USA). For *in vitro* activation, T cells from patients with AIH and buffy coat were magnetic sorted using Human Pan T cell Isolation Kit (Miltenyi Biotec, German) and subsequently incubated with  $\alpha$ -CD3/CD28 beads (Miltenyi Biotec, Germany). To induce differentiation of T helper cells, naïve CD4<sup>+</sup> T cells were purified using Human CD4<sup>+</sup> Naïve T cell Isolation Kit II (Miltenyi Biotec, German) and activated with  $\alpha$ -CD3/CD28 beads. To induce Tregs,  $\alpha$ -CD3/CD28 beads, 5 ng/mL of TGF $\beta$  and 20 U/L IL-2 were applied. For polarization of Th1 cells, naïve CD4<sup>+</sup> T cells were cultured with  $\alpha$ -CD3/CD28 beads, 2 ng/mL IL-12 and 5  $\mu\text{g/mL}$  anti-IL-4 mAb. For Th17 induction, cells were cultured with  $\alpha$ -CD3/CD28 beads, 10 ng/mL IL-1 $\beta$ , 10 ng/mL IL-6, 20 ng/mL IL-23, 5 ng/mL TGF- $\beta$ , 5  $\mu\text{g/mL}$  anti-IL-4 mAb, and 5  $\mu\text{g/mL}$  anti-IFN- $\gamma$  mAb. After 3-day culture, T cells were re-stimulated with phorbol 12-myristate 13-acetate (PMA), ionomycin and brefeldin Leukocyte

(Activation Cocktail with BD GolgiPlug<sup>TM</sup>, BD Bioscience) for another 5 hours before intracellular staining of cytokines.

### **Transcriptional sequencing**

Human primary T cells were sorted from buffy coat, activated with  $\alpha$ -CD3/CD28 beads and simultaneously treated with ICA 0.25mM or vehicle for 16 hours before transcriptional sequencing. Details are provided in Supplementary Methods.

### **Transfection of primary human T cell**

Negative control and shRNA knockdown virus carried with green fluorescent protein (GFP) tags were purchased from HANBIO (Shanghai, China). Briefly, primary human T cells were sorted and plated with  $\alpha$ -CD3/CD28 beads for 16 hours. Then, the lentivirus was added into the pre-activated T cells and the plate was spun at 1000 $\times$ g for 90 min. Then, the T cells and lentivirus were co-cultured overnight at 37°C before refreshing the medium. After that, the infected T cells were activated with the presence of ICA or vehicle for additional 72 hours. For flow cytometry, GFP-positive T cells were gated for further examination.

### **ChIP assay**

ChIP experiments were performed with Chromatin Immunoprecipitation (ChIP) Assay Kit (#17--295, Merck Millipore) according to the manufacturer instructions. Briefly, primary human T cells were purified and activated with the presence of ICA (0.25 mM). After 4 hours of culture, cells were fixed with 1% formaldehyde. Chromatin was sheared by sonication using Bioruptor Pico (Belgium) and the supernatant fraction was diluted. Each sample was incubated with 5  $\mu$ g of anti-AhR antibody (D5S6H, Cell Signaling) or IgG isotype control (DA1E, Cell Signaling) overnight at 4°C with rotation, and then with Protein A Agarose/Salmon Sperm DNA for another 1 hour. Quantitative PCR was adopted to amplify the DNA fragments after reversing crosslinking, and finally the productions of qPCR were confirmed by gel electrophoresis. The primer sequences for ChIP-qPCR were as follows: Pik3ip1 primer 1, forward-5'-TGCAGGTGATTGAACGACCA-3,' reverse-5'-TGATCGGCTGCTAAGCACAA-3'; Pik3ip1 primer 2, forward-5'-CAGTGCTCCTTGTCCATCCCTTG-3,' reverse-5'-GCCATCCCTTGACCTGCTTTACC-3.' The results of qPCR were normalized to input signals.

### **Mice**

Wild type (WT) C57BL/6J were purchased from the Shanghai SLAC laboratory Animal Co. Ltd. AhR<sup>loxP</sup> (B6.129(FVB)-*Ahr*<sup>tm3.1Bra/J</sup>) mice were kindly provided by professor Yufeng Zhou (Children's Hospital and Institutes of Biomedical Sciences, Fudan University). CD4-Cre mice (Tg(Cd4-cre)1Cwi/BfluJ) were purchased from Shanghai Model Organisms (Shanghai, China). AhR<sup>loxP</sup> mice and CD4-Cre mice were maintained on a C57BL/6 background and were crossed for CD4-specific deletion of AhR (AhR<sup>fl/fl</sup>Cd4-Cre). All the mice were housed under specific pathogen-free (SPF) environment at the animal facility of Renji Hospital, School of Medicine, Shanghai Jiao Tong University.

### **ConA-induced hepatitis and treatment of ICA**

To induce immune-mediated hepatitis, female mice aged 8–10 weeks were intravenously injected with PBS or 10 mg/kg Con A (Sigma-Aldrich, USA). For supplementation of indole derivatives, ICA (Sigma-Aldrich, USA) was delivered at a dose of 50 mg/kg/day in a final mixture of DMSO (20%), PEG400 (40%) and citric acid (2%).<sup>24</sup> ICA treatment was started 48 hours prior to ConA and administrated daily by intraperitoneal injection. Mice were sacrificed 16 hours following Con A challenge to examine tissue injury, serum alanine aminotransferase (ALT) and aspartate aminotransferase (AST).

## **AAV IL-12 model and treatment of ICA**

Adeno-associated virus (AAV) vectors and AAV8 particles were produced by Obio Technology (Shanghai, China), as previously described methods.<sup>25</sup> The AAV 8 vector was constructed with a transgene encoding signal-chain IL-12 and transcriptionally regulated by the chimeric albumin promoter to guarantee liver-specific expression of IL-12. To induce autoimmune hepatitis, C57BL/6 mouse was administered AAV IL-12 i.v. at a dose of  $5 \times 10^{10}$  viral genomes/kg and sacrificed at 4 weeks. AAV8 vector constructed with a transgene encoding luciferase was used as control. For supplementation of indole derivatives, ICA (Sigma-Aldrich, USA) was orally delivered at a dose of 100 mg/kg/day every other day.

## **Administration of *Lactobacillus reuteri***

*Lactobacillus reuteri* (100–23) was purchased from CICC (Beijing, China) and was cultured in de Man, Rogosa and Sharpe (MRS) broth at 37°C under anaerobic conditions. For microbial intervention experiments, mice were fed with tryptophan-high diet (1.19%) and gavaged with  $2 \times 10^9$  colony-forming units (CFUs) of live *L.reuteri* in 100 µL PBS every other day. The control group underwent standard chow (0.28% tryptophan) and was gavaged with PBS.

## **Statistics**

All statistical analyses were performed using Graphpad Prism software (version 9.0) and R statistical software (version 4.2.2). Data were presented as the mean  $\pm$  standard error (SEM). Statistical differences were determined by two-tailed Student's *t*-test for comparisons in independent experiments. Mann–Whitney test was used for comparisons of microbial metabolites between patients with AIH and healthy controls. Spearman correlation analysis was performed to examine the relevance between ICA and clinical variables. Significance was defined as \**p* < 0.05, \*\**p* < 0.01 and \*\*\**p* < 0.001.

## **Study approval**

For human samples, the study was conducted in accordance with the Declaration of Helsinki and the procedures were reviewed and approved by the Ethics Committee of Renji Hospital, School of Medicine, Shanghai Jiao Tong University (#2013–030). All animal experiments were performed in accordance and with the approval of Institutional Animal Care and Use Committee of Shanghai Jiao Tong University.

## **Results**

### **Level of indole-3-carboxaldehyde is reduced in patients of AIH**

To investigate the outputs of microbial tryptophan metabolism, we quantified indole derivatives in individuals with AIH (*n* = 42) and matched healthy controls (*n* = 34) using UHPLC-MS/MS. The patients with AIH have not been treated with steroids. Intriguingly, we identified that fecal concentrations of indole-3-carboxaldehyde (ICA) were markedly lower in patients with AIH than healthy controls ( $3.608 \pm 0.5803$  vs  $2.020 \pm 0.2534$ , *P* < 0.01, [Figure 1\(A\)](#)). There was no difference in concentrations of indole-3-acetic acid (IAA), indole-3-propionic acid (IPA), or indole-3-lactic acid ([Figure 1\(A\)](#)), as well as other tryptophan metabolites ([Supplementary Figure S1A](#)). Next, we examined the clinical significance of ICA. Levels of ICA were negatively correlated to the biochemical index of patients with AIH, including ALT ( $r = -0.3713$ , *p* = 0.0155, [Figure 1\(B\)](#)), AST ( $r = -0.3141$ , *p* = 0.0482, [Figure 1\(C\)](#)) and AKP ( $r = -0.4473$ , *p* = 0.0030, [Figure 1\(D\)](#)). However, there was no significant association between ICA and the levels of IgG ([Supplementary Figure S1C](#)).

### **Supplementation of ICA in vitro restricts activation of effector T cells**

While the etiology of AIH remains elusive, human studies suggest a central role for the effector T subsets that perpetrate the hepatocyte damage.<sup>2</sup> To investigate the effects of ICA on T cell function, peripheral T cells were purified from patients with AIH and then cultured with  $\alpha$ -CD3/CD28 mAbs and ICA, and subsequently

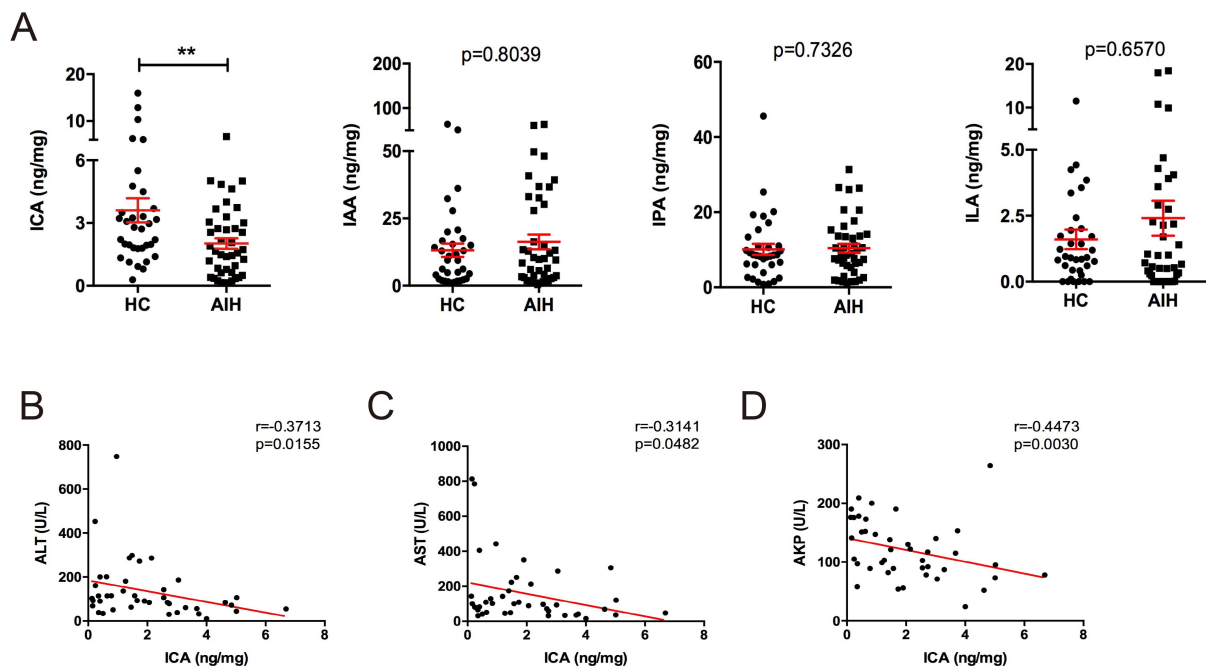


**Figure 1.** Level of indole-3-carboxaldehyde is reduced in patients of AIH. (A) fecal concentrations of ICA, IAA, IPA, ILA in the same cohorts of AIH ( $n = 42$ ) and healthy controls ( $n = 34$ ) as measured by UHPLC-MS/MS. Correlation analysis between fecal ICA and levels of biochemical indexes including (B) ALT, (C) AST and (D) AKP in patients with AIH ( $n = 42$ ). Data are shown as mean  $\pm$  SEM.  $**p < .01$  by Mann–Whitney test. Spearman correlation analysis in Figure B–D. indole-3-carboxaldehyde; AIH, autoimmune hepatitis; IAA, indole-3-acetic acid; IPA, indole-3-propionic acid; ILA, indole-3-lactic acid; UHPLC-MS/MS: ultra-high performance liquid chromatography-tandem mass spectrometry; ALT, alanine transferase; AST, aspartate transferase; ALP, alkaline phosphatase.

analyzed by flow cytometry. Supplementation with ICA significantly downregulated the expression of early activation markers, CD69 and CD25, in both CD4<sup>+</sup> and CD8<sup>+</sup> T cell subsets (Figure 2(A)). Since activation of T cells is marked by effector functions as well as clonal expansion, we then assessed the T cell proliferation using cell-tracing dye CFSE. As a result, ICA significantly inhibited T cell proliferation following stimulation with  $\alpha$ -CD3/CD28 mAbs (Figure 2(B)). In accordance, productions of effector cytokines, including IFN- $\gamma$  and IL-2, were suppressed by ICA treatment (Figure 2(C)).

Next, we explored the effects of ICA on the differentiation of Th cells. Naïve CD4<sup>+</sup> T cells were isolated from patients with AIH and cultured under Th1 and Treg skewing conditions, with or without ICA. We noted that treatment with ICA hampered Th1 polarization, demonstrated by marked reduction in the number of IFN- $\gamma$ -producing CD4<sup>+</sup> T cells (Figure 2(D)). Expression level of Tbet was also downregulated by ICA during Th1 polarization (Figure 2(E)). In addition, *in vitro* treatment of ICA promoted the expansion of CD25<sup>high</sup>Foxp3<sup>+</sup> Tregs (Figure 2(F)). A similar regulatory effect of ICA on Treg and Th1 was confirmed in healthy controls by using buffy coat (Supplementary Figure S2A–D). In line with the previous studies that AhR ligands promoted Th17 differentiation,<sup>26</sup> we observed a slightly enhanced production of IL-17A by ICA (Supplementary Figure S2E, F). Taken together, *in vitro* culture of T cells suggests that intervention of ICA may limit the T cell-mediated immune attack involved in disease pathogenesis.

### ICA upregulates *Pik3ip1* expression and modulates T cell homeostasis by inhibiting PI3K/Akt/mTOR signaling

To delineate the ICA-elicited transcriptional changes, we performed RNA sequencing on primary human T cells activated in the presence of ICA. Compared to the vehicle group, ICA-treated T cells showed upregulation of 272 genes and downregulation of 291 genes ( $\text{Log}_2(\text{Fold change}) > 1$ ,  $\text{FDR} < 0.01$ , Figure 3(A)). Enrichment analysis

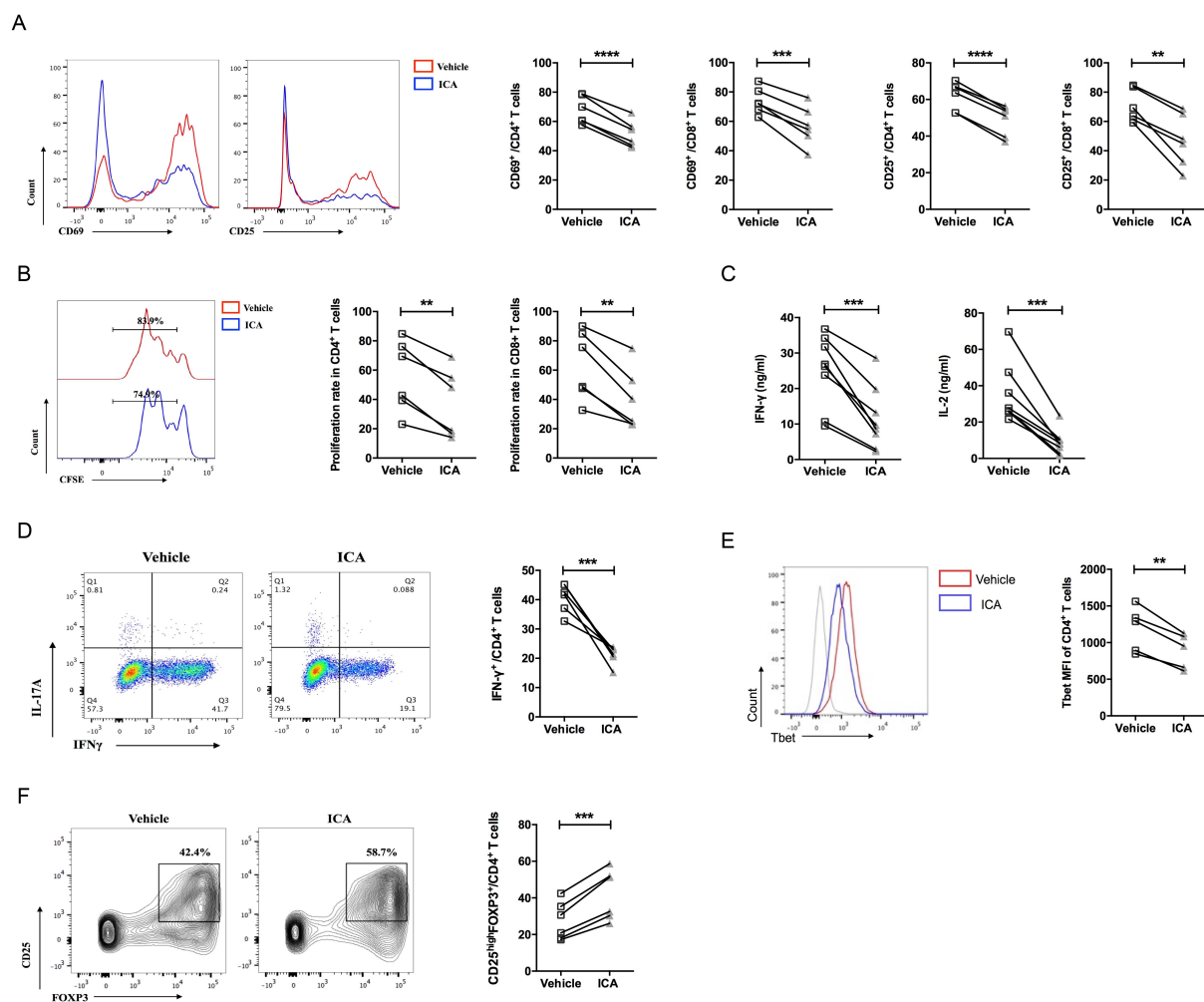


**Figure 2.** Treatment of ICA restricts activation of effector T cells. (A) Representative flow cytometry plots and statistical analyses of expression levels of CD25 and CD69 on peripheral T cells from patients with AIH ( $n = 6$ ) after being incubated with  $\alpha$ -CD3/CD28 mAbs and ICA (250  $\mu$ M) or vehicle for 36 hours. (B) Representative flow cytometry plots and statistical analyses of CFSE assessing the proliferation of peripheral T cells sorted from patients with AIH ( $n = 6$ ) incubated with  $\alpha$ -CD3/CD28 mAbs and ICA (250  $\mu$ M) or vehicle for 72 hours. (C) ELISA measurement of IFN- $\gamma$  and IL-2 secreted by T cells from patients with AIH ( $n = 6$ ) incubated with  $\alpha$ -CD3/CD28 mAbs and ICA (250  $\mu$ M) or vehicle for 36 hours. Representative flow cytometry plots and statistical analyses of (D) frequency of IFN- $\gamma$ -producing CD4<sup>+</sup> T cells ( $n = 6$ ) and (E) expression of tbet ( $n = 5$ ) treated with or without ICA (250  $\mu$ M) under the polarizing condition of Th1. (F) representative flow cytometry plots and statistical analyses of frequency of Treg (CD4<sup>+</sup>CD25<sup>high</sup>FOXP3<sup>+</sup>) induced with or without ICA (250  $\mu$ M) under the polarizing condition of Treg ( $n = 6$ ). Data are shown as mean  $\pm$  SEM. \*\* $p < .01$ , \*\*\* $p < .001$  by student's paired t test. ICA, indole-3-carboxaldehyde; IFN- $\gamma$ , interferon- $\gamma$ .

revealed that ICA treatment suppressed PI3K-Akt signaling and Akt1-targeted genes (Figure 3(B,C)), which is essential for T cell quiescence exit and metabolic reprogramming.<sup>27–29</sup>

Of note, Pik3ip1, a critical gene in PI3K-Akt pathway, was substantially increased by ICA (Figure 3(A)). Pik3ip1 is highly expressed in immune cells, particularly T lymphocytes, and has been identified as a negative regulator of PI3K<sup>8,20,21</sup>. Thus, we hypothesized that ICA treatment increases Pik3ip1 expression, leading to the suppression of PI3K/Akt/mTOR signaling in antigen-stimulated T cells. To validate this, peripheral T cells were isolated and incubated with ICA. As a consequence, a reproducible upregulated expression of Pik3ip1 in ICA-treated group was observed with or without the stimulation of mimetic signals of TCR and CD28, demonstrated by qPCR and western blot assay (Figure 3(D,E)). In line with the previous study, Pik3ip1 expression declined upon the *in vitro* stimulation of the TCR signal,<sup>19</sup> which was reported to be probably induced by matrix metalloproteases. We next examined the activity of PI3K/Akt/mTOR in primary T cells. Immunoblot analysis confirmed that ICA inhibited phosphorylation of Akt and ribosomal

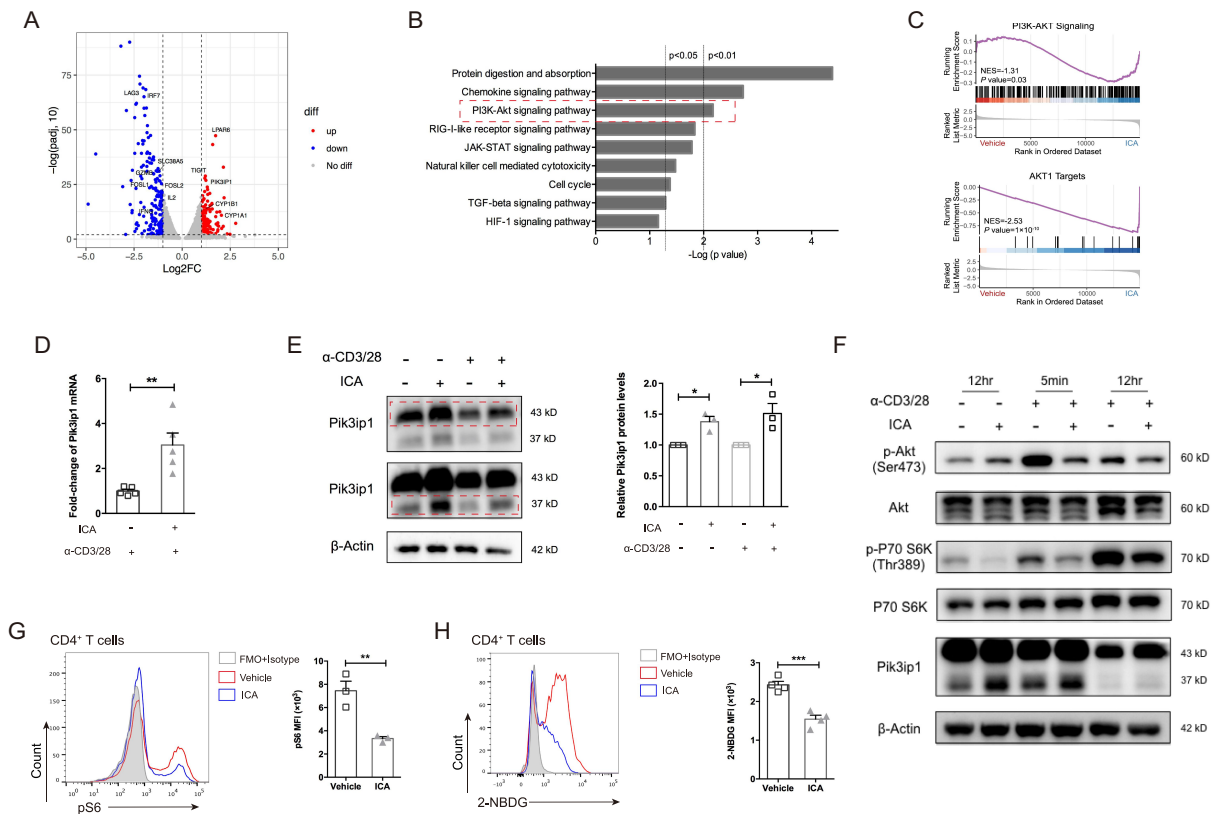


**Figure 3.** ICA upregulates Pik3ip1 expression and suppresses PI3K/Akt/mTOR signaling in T lymphocytes. (A) Volcano plots show global gene-expression profiles of primary human T cells treated with ICA (250  $\mu$ M) or vehicle and stimulated for 16 hours with  $\alpha$ -CD3/CD28 mAbs. Transcripts with a  $\text{Log}_2(\text{Fold change}) > 1$  and  $\text{FDR} < 0.01$  in ICA-treated T cells are shown in red (upregulated, 272 genes) or blue (downregulated, 291 genes). (B) Kyoto encyclopedia of genes and genomes (KEGG) pathways differed between the ICA group and the vehicle group ( $p < 0.05$ ). (C) Gene set enrichment analysis (GSEA) of PI3K-Akt signaling pathway and Akt1 targeted genes. The normalized enrichment (NES) and the  $p$  value are labeled. (D) Fold change of Pik3ip1 mRNA assessed by quantitative PCR in primary human T cells ( $n = 5$ ). (E) treatment of ICA (250  $\mu$ M) increased the expression of Pik3ip1 in T lymphocytes, with or without the stimulation of  $\alpha$ -CD3/CD28 mAbs for 12 hours. The two bands of different exposure time demonstrate a consistent change of Pik3ip1 at 37kDa (the unglycosylated form) and 45kDa (the glycosylated form). The relative quantification of blots intensity was done by comparing the ICA group to the vehicle. (F) After being treated with ICA or vehicle for 16 hr, primary T cells were stimulated with  $\alpha$ -CD3/CD28 mAbs. The indicated proteins involved in PI3K signaling were examined by Immunoblot analysis at indicated timepoints. Flow cytometric analysis of (G) pS6 expression and (H) 2-NBDG levels in  $\text{CD4}^+$  T cells treated with ICA and vehicle and stimulated with  $\alpha$ -CD3/CD28 mAbs for 12 and 36 hours, respectively. Data are shown as mean  $\pm$  SEM. \*\* $p < .05$ , \*\* $p < .01$ , \*\*\* $p < .001$  by two-tailed Student's  $t$  test. Data are representative of three independent experiments (D-H). ICA, indole-3-carbaldehyde; Pik3ip1, PI3K interacting protein 1; Akt, protein kinase B; p70 S6K, ribosomal protein S6K1; S6, ribosomal protein S6; AhR, aryl hydrocarbon receptor.

protein S6K1 (p70 S6K) and simultaneously induced higher expression of Pik3ip1 in T lymphocytes (Figure 3(F)). As a sensitive readout of mTOR activity, phosphorylation of ribosomal protein S6 phosphorylation (pS6) was found to be downregulated in ICA group by flow cytometry (Figure 3(G)). Given that PI3K/Akt/mTOR is a seminal event driving T cell metabolic reprogramming upon activation, we assessed the process of glucose uptake by using 2-NBDG, a fluorescent D-glucose analog. Consistently, intracellular levels of 2-NBDG were significantly lower in ICA-treated T cells compared to the vehicle controls (Figure 3(H)). We further incubated  $\text{CD4}^+$  T cells with ICA and Akt agonist SC-79, to examine whether the regulatory effects of ICA were due to the downregulated PI3K/Akt signaling. As a result, agonism of Akt in ICA-treated group partially restored the release of Th1-cytokines (Supplementary Figure S3A), suggesting that the effects of ICA on the differentiation of Th1 were dependent on suppression of PI3K/Akt pathway. Taken together, we posited that ICA treatment restricted T cell activation by increasing the expression of Pik3ip1, which in turn suppresses the PI3K/Akt/mTOR signaling cascades.

### AhR engaged by ICA transcriptionally activates *Pik3ip1* in T cells

Next, we explored how ICA upregulated *Pik3ip1* expression in T cells. Indole derivatives are known to activate AhR, a ligand-activated transcription factor that plays a pleiotropic role in the maintenance of innate and adaptive immune homeostasis.<sup>30,31</sup> Upon ligand binding, cytoplasmic AhR translocates into the nucleus, where it binds to genomic regulatory regions and transcriptionally modulates target gene expression.<sup>32</sup> First, we observed that incubation with ICA resulted in the translocation of cytoplasmic AhR to the nucleus, as demonstrated by confocal microscopy (Figure 4(A)). The nucleocytoplasmic separation assay showed an elevated ratio of the nuclear AhR to the total contents of AhR upon ICA treatment (Figure 4(B)). Additionally, ICA treatment triggered the transcription of AhR and cytochrome P4501A1 (CYP1A1), an AhR-targeting gene (Figure 4(C,D)), indicating that ICA acts as an AhR ligand in T cells to regulate the targeted genes expression.

To assess the potential binding of AhR to the gene sequences of the *Pik3ip1*, chromatin immunoprecipitation (ChIP) assays were performed in primary T cells sorted from buffy coat. We demonstrated that AhR directly bound to the promoter of *Pik3ip1* gene (Figure 4(E)), suggesting that ICA activates AhR within T lymphocytes and subsequently upregulates *Pik3ip1* expression. Furthermore, we investigated the effects of knockdown of AhR expression using short hairpin (sh)RNA. Importantly, ICA-mediated suppression of PI3K/Akt/mTOR signaling in primary T cells could be partially reversed in the AhR-knockdown groups, as demonstrated by flow cytometry (Figure 4(F,G)) and western blot (Supplementary Figure S3B). These data suggested that AhR is required for the immunoregulatory effects of ICA in T lymphocytes.

### Supplementation of ICA alleviates T cell-mediated hepatitis in murine model

We first used the murine model of ConA-induced hepatitis to explore the role of ICA in the regulation of T cell responses (Figure 5(A)). Induction of hepatitis was evaluated in the vehicle and ICA treatment group by H&E staining of liver tissues (Figure 5(B)). As a result, ICA-treated mice demonstrated mild hepatic necrosis with significantly lower levels of AST and ALT in serum, compared to the vehicle group (Figure 5(C,D)). ELISA measurement showed serum level of IFN- $\gamma$  was largely decreased by ICA in ConA model (Figure 5(E)). Consistent with the *in vitro* data, nuclear translocation of AhR induced by ICA was confirmed *in vivo* (Supplementary Figure S4B). In addition, activation of hepatic T lymphocytes was significantly inhibited by ICA supplementation (Figure 5(F)). However, the frequency of Treg (CD4<sup>+</sup>CD25<sup>+</sup>Foxp3<sup>+</sup>) did not differ between the ICA and control groups (Figure 5(G)), which might be attributed to the alleviated hepatic inflammation in ICA-treated mice. Additionally, to detect the intracellular IFN- $\gamma$ , liver MNCs were freshly isolated and incubated with protein transport inhibitor (Brefeldin A) for 6 h at 37°C to block the release of cytokines. In ConA model, CD4<sup>+</sup> T cells in ICA group displayed apparently lower MFI of IFN- $\gamma$ <sup>+</sup>, compared with the vehicle group (Figure 5(H)). The percentages of IFN- $\gamma$ <sup>+</sup> cells were of relatively low levels, as the polyclonal activator (PMA) was not used to reactivate T cells (Supplementary Figure S4C). In parallel, less proportions of TNF- $\alpha$ <sup>+</sup> and IL-17A<sup>+</sup>-producing effector CD4<sup>+</sup> T cells were observed in ICA-treated mice (Supplementary figure S4D, E). However, there is no significant difference in hepatic CD8<sup>+</sup> T cell, NK and NKT cells with regard to the release of IFN- $\gamma$  (Supplementary figure S4F-H). In line with the *in vitro* data, ICA-treated mice exhibited significantly higher levels of *Pik3ip1* on hepatic T cells than controls, as demonstrated by qPCR and flow cytometry (Figure 5(I,J)). Furthermore, the phosphorylation level of S6 in T lymphocytes was also downregulated by ICA treatment *in vivo* (Figure 5(K), Supplementary figure S4J, K), suggesting an inhibition of mTOR signaling. Serum level of IL-22, previously reported to be boosted by AhR agonism,<sup>31</sup> was not different between the two groups (Supplementary figure S4I). We also performed cytometry flow analysis of hepatic mononuclear cells, production of IL-22 within liver was minimal and there was no elevation upon treatment of ICA (data not shown), suggesting that the protective role conferred by ICA here was not associated with AhR-IL-22 axis.

We next used an adeno-associated virus (AAV) IL-12 mouse model to validate the therapeutic role of ICA in AIH (Figure 5(L)). Infiltration of T lymphocytes was recognized to play pathogenic roles in this model triggered by liver-specific expression of IL-12.<sup>25</sup> Interface hepatitis, elevation of ALT and autoantibodies, which mimic the characteristics of autoimmune hepatitis, have been confirmed in this model in previous work.<sup>25</sup> Consequently, supplementation of ICA ameliorated hepatic inflammation and tissue

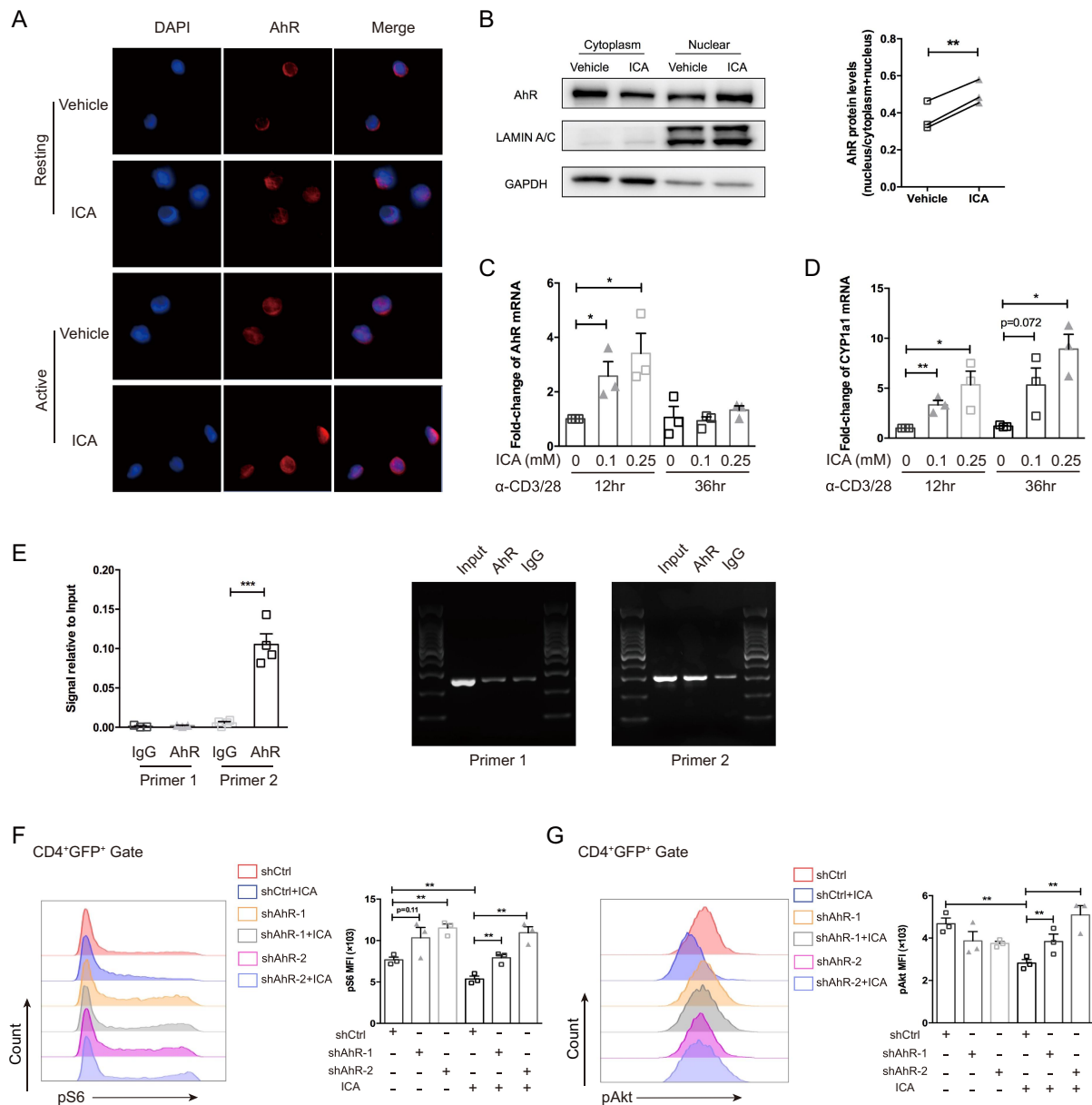


**Figure 4.** AhR engaged by ICA transcriptionally activates *Pik3ip1* in T cells. (A) Human peripheral T cells were immunostained for AhR after being stimulated with ICA (250  $\mu$ M) and  $\alpha$ -CD3/CD28 mAbs overnight. (B) The T cells incubated with ICA or vehicle and activated for 24 h were fractionated, and the cytoplasmic and nuclear protein fractions were then blotted for AhR, LAMIN A/C and GAPDH. The representative blots and quantification of AhR protein levels (ratio of the nuclear to the total AhR) are shown. T cell transcription of (C) AhR and (D) its downstream CYP1A1 at indicated timepoints were analyzed by qPCR. (E) ChIP analysis of the interaction between AhR and *Pik3ip1* gene in primary human T cells activated with  $\alpha$ -CD3/CD28 mAbs. Primer 2 is designed with the promoter sequences of *Pik3ip1*, and the negative control primer 1 corresponds to the 3' non-coding region of *Pik3ip1*. The productions of qPCR were confirmed by gel electrophoresis. (F, G) Representative flow cytometry plots and statistical analyses of the phosphorylated levels of S6 and Akt in human primary T cells infected with lentivirus containing AhR-specific shRNA or scramble shRNA. The infection rate of lentivirus was about 40–50%, and GFP<sup>+</sup> T cells were gated before analysis. Data are shown as mean  $\pm$  SEM. \*\* $p < .05$ , \*\*\* $p < .01$  by two-tailed student's t test. Data are representative of three independent experiments (A-G). ICA, indole-3-carbaldehyde; AhR, aryl hydrocarbon receptor; CYP7A1, cholesterol 7 $\alpha$ -hydroxylase; S6, ribosomal protein S6; Akt, protein kinase B; shRNA, short-hairpin RNA.

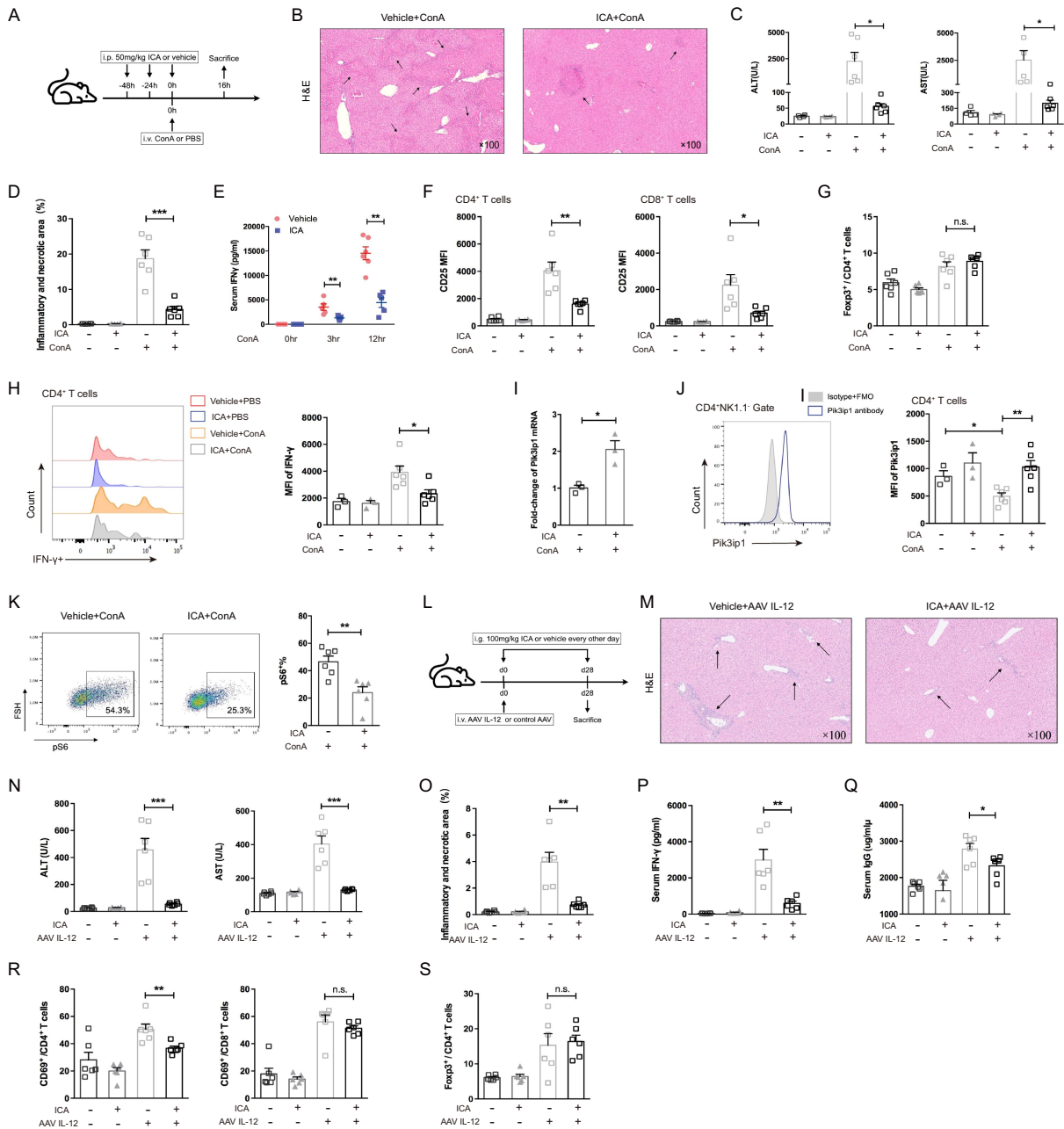


**Figure 5.** Supplementation of ICA mitigated T cell-mediated hepatitis. (A) Experimental design of ConA model and ICA supplementation schedule. (B) Representative H&E staining ( $\times 100$ ) of livers in mice treated with vehicle or ICA intraperitoneally and subjected to ConA challenge for 16 hours. (C) Serum levels of ALT and AST in vehicle- and ICA-treated groups ( $n = 4-6$  per group). (D) Quantification of inflammatory and necrotic area. (E) IFN- $\gamma$  detected by ELISA at indicated timepoints after ConA injection. (F) statistical analyses of expression levels of CD25 in hepatic CD4 $^+$  T cells and CD8 $^+$  T cells. (G) Statistical analyses of the hepatic frequency of Tregs (CD4 $^+$ NK1.1 $^-$ FOXP3 $^+$ ). (H) Representative flow cytometry plots and statistical analyses of IFN- $\gamma$  $^+$  MFI in hepatic CD4 $^+$  T cells in vehicle and ICA-treated groups. For detection of intracellular cytokines after ConA challenge, HMNCs were freshly isolated and treated with brefeldin A for 6 hours at 37°C to block cytokine release. (I) Quantitative PCR results of Pik3ip1 in hepatic T lymphocytes. (J) flow cytometry analyses of Pik3ip1 expression in hepatic T cells. (K) Representative flow cytometry plots and statistical analyses of the phosphorylation level of S6 in hepatic T cells. (L) experimental design of AAV IL-12 models and ICA supplementation schedule. (M) representative H&E staining ( $\times 100$ ) of livers in mice administered with AAV IL-12 and treated with vehicle or ICA for 4 weeks. (N) Serum levels of ALT and AST in vehicle- and ICA-treated AAV IL-12 mice ( $n = 6$  per group). (O) quantification of inflammatory and necrotic area. (P) ELISA measurement of serum IFN- $\gamma$ . (Q) ELISA measurement of serum IgG. Statistical analyses of (R) activated CD4 $^+$  T cells and CD8 $^+$  T cells and (S) hepatic Tregs (CD4 $^+$ NK1.1 $^-$ FOXP3 $^+$ ) in mice administered with AAV luc (control AAV) or AAV IL-12 and being treated with or without ICA. Data are shown as mean  $\pm$  SEM. \*\* $p < .05$ , \*\*\* $p < .01$  by two-tailed student's t test. Data are representative of at least two independent experiments. ICA, indole-3-carbaldehyde; ConA, concanavalin A; ALT, alanine aminotransferase; AST, aspartate aminotransferase; IFN- $\gamma$ , interferon- $\gamma$ ; Pik3ip1, PI3K interacting protein 1; AAV, adenovirus-associated virus.

damage upon in AAV IL-12 model based on the results of histological and serological analyses (Figure 5 (M-O)). Consistent with the results from ConA model, production of IFN- $\gamma$  was significantly reduced by ICA administration (Figure 5(P)). In parallel, levels of IgG were elevated in AAV IL-12 model and decreased upon ICA treatment (Figure 5(Q)). Further dissection of hepatic T cell compartment revealed that ICA suppressed overactivation of CD4<sup>+</sup> T cells, while the frequency of Treg was not impacted (Figure 5(R,S)). Collectively, administration of ICA rendered mice resistant to the T cell-mediated hepatitis.

### Amelioration of hepatitis by ICA requires T cell expression of AhR

To test whether AhR in T cells was responsible for the anti-inflammatory effects of ICA, we generated mice with AhR T cell-conditional knockout (AhR<sup>fl/fl</sup>Cd4-Cre) mice by crossing AhR<sup>fl/fl</sup> mice with Cd4-Cre mice. In the vehicle groups, hepatic necrosis and inflammatory infiltration were comparable between AhR<sup>fl/fl</sup> and AhR<sup>fl/fl</sup>Cd4-Cre mice. However, in the ICA-supplemented groups, AhR<sup>fl/fl</sup>Cd4-Cre mice exhibited marked aggravated tissue damage, as well as higher levels of transaminases compared to AhR<sup>fl/fl</sup> control (Figure 6(A-C)). Consistently, ICA was not capable to mitigate the activation of hepatic CD4<sup>+</sup> and CD8<sup>+</sup> T cell in AhR<sup>fl/fl</sup>Cd4-Cre mice subjected to ConA (Figure 6 (D)). Collectively, these data suggested that ICA regulated T cell immunity and protected mice from immune-mediated hepatitis in an AhR-dependent manner.

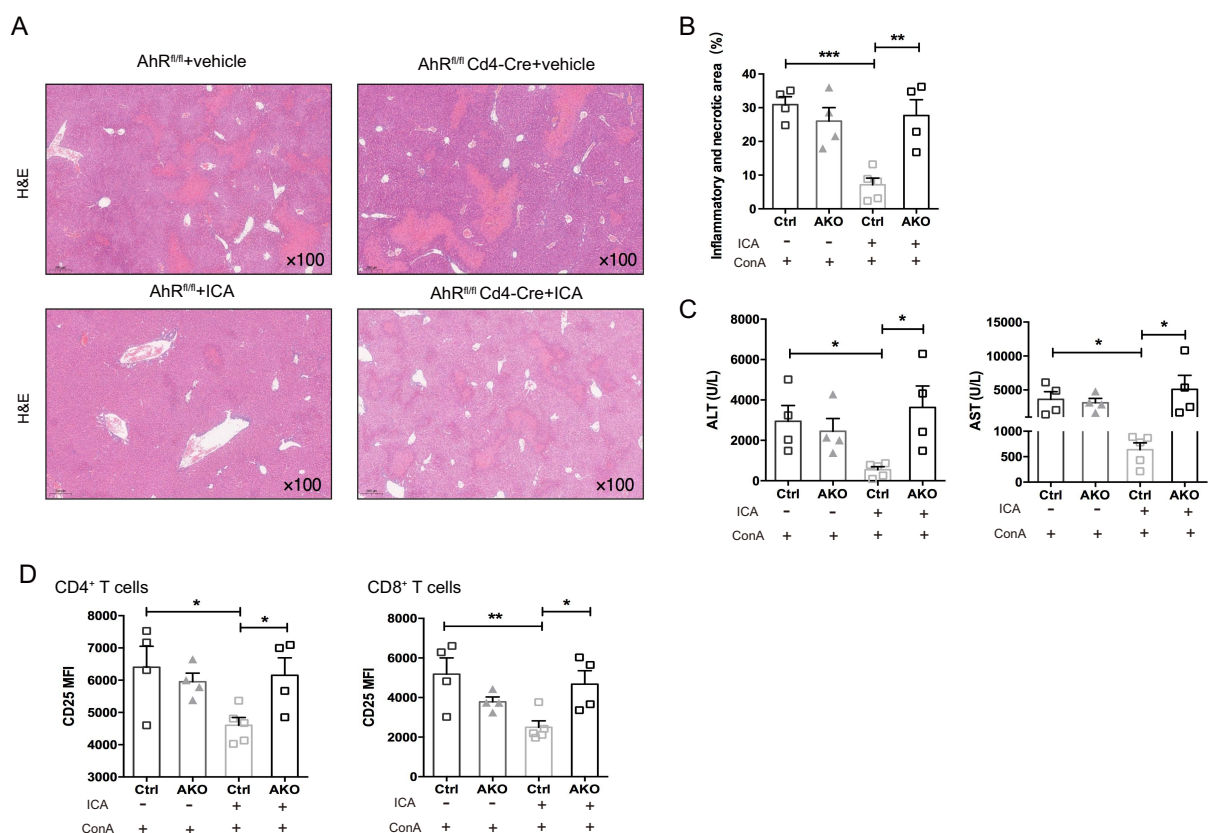


**Figure 6.** Amelioration of hepatitis by ICA supplementation requires T cell expression of AhR. (A) representative H&E staining ( $\times 100$ ) of livers in AhR<sup>fl/fl</sup> and AhR<sup>fl/fl</sup> Cd4-Cre mice treated with vehicle or ICA intraperitoneally and subjected to ConA challenge. (B) quantification of inflammatory and necrotic area in each group ( $n = 4-5$  per group). (C) serum levels of ALT and AST, respectively. (D) statistical analyses of expression levels of CD25 in hepatic CD4<sup>+</sup> T cells and CD8<sup>+</sup> T cells in AhR<sup>fl/fl</sup> and AhR<sup>fl/fl</sup> Cd4-Cre mice treated with vehicle or ICA. Ctrl group refers to the AhR<sup>fl/fl</sup> mice, and AKO refers to AhR<sup>fl/fl</sup> Cd4-Cre mice. Data are shown as mean  $\pm$  SEM.  $^{***}p < .001$ ,  $^{**}p < .01$ ,  $^{*}p < .05$  by two-tailed Student's t test. Data are representative of two independent experiments (A-D). ICA, indole-3-carbaldehyde; AhR, aryl hydrocarbon receptor; ALT, alanine aminotransferase; AST, aspartate aminotransferase.

## Lactobacillus reuteri enhanced levels of ICA and ameliorated immune hepatitis

Lactobacillus reuteri (*L. reuteri*) has been reported to metabolize tryptophan and produce indole derivatives.<sup>33,34</sup> We therefore set out to assess whether supplementation of *L. reuteri* could increase the level of ICA and achieve therapeutic effects (Figure 7(A)). Given that *L. reuteri* catabolizes dietary tryptophan (Trp) into AhR ligands, C57BL/6 mice were provided with a Trp-high (1.19%) diet and orally administered with *L. reuteri*.<sup>35</sup> We confirmed that supplementation of *L. reuteri* *in vivo* induced enrichment of ICA (Figure 7(B)) and was sufficient to mitigate immune hepatitis induced by ConA, as evidenced by histological and serological changes (Figure 7(C-E)). Consistently, mice treated with *L. reuteri* contained lower amount of IFN- $\gamma$  (Figure 7F) and displayed less activated T lymphocytes in liver (Figure 7(G)). Similarly, we applied Trp-enriched diet and *L. reuteri* in AAV IL-12-challenged mice (Figure 7(H)). Amelioration of hepatic inflammation by the probiotic intervention was validated in this chronic hepatitis model (Figure 7(I,J)). By means of flow cytometry, we observed dampened activation of CD4<sup>+</sup> and CD8<sup>+</sup>

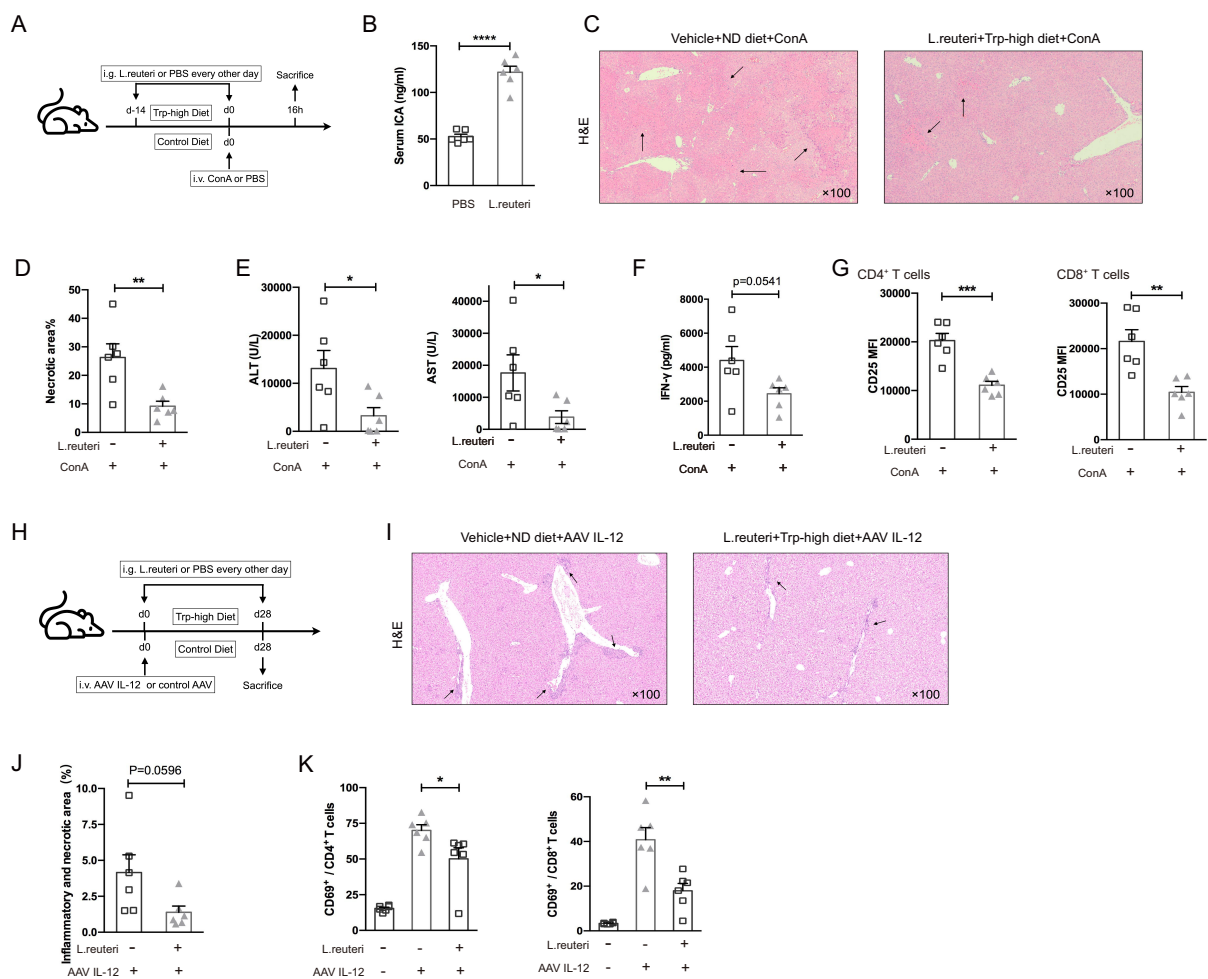


**Figure 7.** Lactobacillus reuteri enhanced levels of ICA and ameliorated immune hepatitis. (A) experimental design of ConA-induced hepatitis in C57BL/6 mice and *L. Reuteri* administration schedule. (B) Serum concentrations of ICA in mice administered with *L. Reuteri* or PBS as measured by UHPLC-MS/MS. (C) Representative H&E staining ( $\times 100$ ) of livers in mice orally gavage of *L. Reuteri* or PBS and subjected to ConA challenge. (D) Quantification of inflammatory and necrotic area in each group ( $n = 6$  per group). (E) Serum levels of ALT and AST. (F) ELISA measurement of serum IFN- $\gamma$ . (G) Statistical analyses of expression levels of CD25 in hepatic CD4<sup>+</sup> T cells and CD8<sup>+</sup> T cells. (H) Experimental design of AAV IL-12 models and *L. Reuteri* administration schedule. (I) representative H&E staining ( $\times 100$ ) of livers. (J) Quantification of inflammatory and necrotic area in each group ( $n = 6$  per group). (K) Statistical analyses of expression levels of CD69 in hepatic CD4<sup>+</sup> T cells and CD8<sup>+</sup> T cells. Data are shown as mean  $\pm$  SEM. \*\* $p < .05$ , \*\*\* $p < .01$ , \*\*\*\* $p < .0001$  by two-tailed student's t test. Data are representative of two independent experiments (D-K).

T cells in *L. reuteri*-treated group (Figure 7(K)). Taken together, we showed that combination of dietary and probiotic therapy could increase the abundance of ICA and exert protective effects on immune hepatitis.

## Discussion

In the current study, we report that patients with AIH exhibited reduced level of ICA, a commensal metabolite derived from tryptophan. We demonstrate that administration of ICA or tryptophan-metabolizing bacteria ameliorated immune hepatitis by suppressing effector T cell subsets. Mechanistically, treatment of ICA activated the transcriptional receptor AhR in T cells and thereby enhanced Pik3ip1 expression. These findings provided proof of principle that supplementation of ICA may serve as a potential immunotherapy to prevent or ameliorate the course of AIH.

Alterations in taxonomic composition have been recently described in autoimmune liver diseases.<sup>9,10,35</sup> Despite many associations, the molecular mechanisms by which microbe interacts with the host remain poorly defined. The byproducts of microbiota metabolites serve as important signals to regulate host physiology in extra-intestinal organs.<sup>14,36</sup> Among the metabolites repertoire, indole derivatives, produced by a large number of commensal bacteria, demonstrate aryl hydrocarbon receptor (AhR) agonistic capacities.<sup>30,31,33</sup> As a cytoplasmic receptor, AhR senses and integrates diverse environmental clues, and in turn functions as a transcription factor to confer immune tolerance locally at the epithelial barrier and systematically.<sup>30,31</sup> Longhi et al. have recently reported that in patients with AIH, an impaired upregulation of CD39 in T cells might be attributed to the aberrant inhibition of AhR by high levels of AHRR and HIF-1 $\alpha$ .<sup>17</sup> Herein, we sought to interpret the imbalance between regulatory and effector T lymphocytes of AIH from the perspectives of gut dysbiosis. We assumed that the impairment of immune tolerance and the inflammation in AIH were partially related to the deficient bacteria-derived tryptophan metabolites and resultant alterations of AhR pathway.

Animal experiments have provided incremental evidence that supplementation of indole derivatives could modify the immune reactions and lead to disease improvement. For instance, exogenous administration of ICA has been shown to reduce graft-versus-host disease via suppressing Type I IFNs signaling.<sup>37</sup> Bacteria-derived indoles were found to be decreased in NAFLD and alcoholic hepatitis, and compensatory administration of AhR agonists reversed liver pathology through boosting IL-22 production.<sup>38,39</sup> Gavage of *L. reuteri* leads the bacteria translocating to the tumor and releasing ICA, which locally potentiates anti-tumor immunity by CD8<sup>+</sup> T cells.<sup>40</sup> In addition to the animal data, immunoregulatory effects conferred by microbial metabolites have been observed in human subjects.<sup>41</sup> Therefore, it is conceivable that correcting the ICA deficiency in patients with AIH may be of therapeutic value.

Indole derivatives are potential agonists of AhR. However, AhR exerted opposing effects in driving either inflammatory or tolerogenic T cell responses depending on the specific AhR ligands and other unknown environmental factors.<sup>26,42</sup> In the current study, we demonstrated that ICA exerted predominantly immunoregulatory effects on Th1 cells and cytotoxic T cells. It is known that TNF- $\alpha$ - and IFN- $\gamma$ -producing Th1 cells are aberrantly expanded in the liver of patients with AIH. Th1 cells pathogenically react with the mimic autoantigen LKM-1.<sup>43,44</sup> Although Th17 and Treg are recognized as subsets with selectively higher expression of AhR, it has also been reported that CD4<sup>+</sup> T helper subsets can generate adequate responses in the presence of AhR agonists.<sup>45</sup> In our experiments, although treatment of ICA promoted expansion of Treg *in vitro*, frequency of hepatic Treg did not differ in ConA or AAV IL-12 models. AhR-activating ligands were previously reported to alleviate murine arthritis by lowering the threshold for Breg induction in response to inflammation, while the frequency of Breg maintained unchanged.<sup>46</sup> The *in vivo* environment is far more complex as other immune cells and cytokine profiles, such as TGF- $\beta$  and IL-6, also impact the Treg differentiation. The inflammation elicited by ConA and AAV IL-12 intrinsically promoted the expansion of Treg. We speculate that the less pro-inflammatory milieu in ICA-treated group might limit the generation of inhibitory cells. Nonetheless, the mitigated liver damage by ICA herein was mainly attributed to the restriction of T cell overactivation. Another issue that should be noted is that myeloid cells and parenchymal cells are also AhR-expressing cells.<sup>30</sup> We therefore confirmed the role of T lymphocytes by showing that T-cell conditional knockout of AhR abrogated the ICA-mediated remission of hepatitis.

Pik3ip1 is a transmembrane protein preferentially expressed on T lymphocytes, particularly naïve T cells.<sup>8,20</sup> Downregulation of Pik3ip1 in T cells has been reported to be prevalent in various autoimmune

disorders including systemic lupus erythematosus, rheumatoid arthritis and multiple sclerosis.<sup>22</sup> With an intracellular motif homologous to the PI3K regulatory subunit p85, Pik3ip1 interferes the PI3K/Akt/mTOR signaling in T cells.<sup>19–21</sup> Accumulating evidence highlights PI3K/Akt/mTOR activation as a seminal event for quiescence exit of naïve T cells and a fundamental determinant in effector T cells differentiation.<sup>29,47</sup> Additionally, it was recently reported that downregulation of Pik3ip1 results in exaggerated activation of T cells and aggravated immune diseases through metabolic reprogramming.<sup>22</sup> In this study, an accordant upregulation of Pik3ip1 by ICA was observed with or without TCR stimulation. We further demonstrated the direct regulation of Pik3ip1 transcription by AhR using ChIP assay and the reverted T cell phenotypes via agonism of Akt. Therefore, we assume that by upregulating Pik3ip1, AhR acts as a rheostat for T cell immunity, which enhances the threshold for effector T cell activation under hepatic inflammatory conditions.

In conclusion, our data demonstrate that gut-microbiota-derived ICA ameliorates liver inflammation through activating AhR in T lymphocytes and subsequently upregulating Pik3ip1. We further show that combination of dietary and probiotic therapeutics increases the level of ICA and prevents from immune-mediated hepatitis. Nonetheless, clearly sufficient bioavailability and safety of indole derivatives in patients require extensive testing in future.

## Acknowledgments

We thank the patients and controls who participated in the study.

## Authorship contributions

XM and RT conceptualized and supervised the study. XM, RT, ZY, YW and BL acquired funding. ZY, QM, XX, ML, ZW and YZ managed the resources. QW, YW, QL and YL collected the samples. BL, YL and XL developed the methodology. BL, YL, XL and JZ performed the experiments. BL wrote the manuscript. RT, XM, YZ and MEG reviewed and edited the manuscript.

## Disclosure statement

No potential conflict of interest was reported by the author(s).

## Funding

This work was supported by the National Natural Science Foundation of China grants (#82200595 to BL, #82270554, 82470558 and 81922010 to RT, #82400608 to YL, #82330018, 82130017 and 81830016 to XM; #82270553 to ZY #82300610 to JZ; #82000532 to YW), Shanghai Natural Science Foundation (#24ZR1444800) and China Postdoctoral Science Foundation (#2024M762050), Innovative research team of high-level local universities in Shanghai (#SHSMU-ZDCX20210301 to XM and #SHSMU-ZLCX20211600 to ZY) and Shanghai Municipal Education Commission-Gaofeng Clinical Medicine Grant Support (#20161311 to RT).

## ORCID

Xiong Ma  <http://orcid.org/0000-0001-9616-4672>

## Data availability statement

The datasets generated during this study are available from the corresponding author on request.

## List of Abbreviations

AIH	autoimmune hepatitis;
AhR	aryl hydrocarbon receptor;
ALP	alkaline phosphatase;
ALT	alanine aminotransferase;
AST	aspartate aminotransferase;
Akt	protein kinase B;
CYP7A1	cholesterol 7 $\alpha$ -hydroxylase;
ChIP	chromatin immunoprecipitation;
ConA	concanavalin A;
DMSO	dimethyl sulfoxide;
IgG	immunoglobulin G;
IFN- $\gamma$	interferon- $\gamma$ ;
IAA	indole-3-acetic acid;
ICA	indole-3-carbaldehyde;
IPA	indole-3-propionic acid;
LMNCs	liver mononuclear cells;
mTOR	mammalian target of rapamycin;
MFI	mean fluorescence intensity;
NK cell	natural killer cell;
NKT cell	natural killer T cell;
PXR	pregnane X receptor;
PI3K	phosphoinositide-3 kinase;
p70 S6K	ribosomal protein S6K1;
Pik3ip1	PI3K interacting protein 1;
PBS	phosphate buffered saline;
SCFAs	short-chain fatty acids;
S6	ribosomal protein S6;
Treg	regulatory T cell; Th cell, helper T cell;
TNF- $\alpha$	Tumor Necrosis Factor- $\alpha$ ;
UHPLC-MS/MS	ultra-high performance liquid chromatography-tandem mass spectrometry.

## References

1. Mieli-Vergani G, Vergani D, Czaja AJ, Manns MP, Krawitt EL, Vierling JM, Lohse AW, Montano-Loza AJ. Autoimmune hepatitis[J]. *Nat Rev Dis Primers*. 2018;4(1):18017. doi: [10.1038/nrdp.2018.17](https://doi.org/10.1038/nrdp.2018.17).
2. Webb GJ, Hirschfield GM, Krawitt EL, Gershwin ME. Cellular and molecular mechanisms of autoimmune hepatitis. *Annu Rev Pathol*. 2018;13(1):247–292. doi: [10.1146/annurev-pathol-020117-043534](https://doi.org/10.1146/annurev-pathol-020117-043534).
3. Longhi MS, Zhang L, Mieli-Vergani G, Vergani D. B and T cells: (still) the dominant orchestrators in autoimmune hepatitis. *Autoimmun Rev*. 2024;23(7–8):103591. doi: [10.1016/j.autrev.2024.103591](https://doi.org/10.1016/j.autrev.2024.103591).
4. Arenz M, Meyer Zum Büschenfelde KH, Löhler HF. Limited T cell receptor V $\beta$ -chain repertoire of liver-infiltrating T cells in autoimmune hepatitis. *J Hepatol*. 1998;28(1):70–77. doi: [10.1016/S0168-8278\(98\)80204-3](https://doi.org/10.1016/S0168-8278(98)80204-3).
5. Yoshizawa K, Ota M, Katsuyama Y, Ichijo T, Inada H, Umemura T, Tanaka E, Kiyosawa K. T cell repertoire in the liver of patients with autoimmune hepatitis. *Hum Immunol*. 1999;60(9):806–815. doi: [10.1016/S0198-8859\(99\)00058-0](https://doi.org/10.1016/S0198-8859(99)00058-0).
6. Liberal R, de Boer YS, Heneghan MA. Established and novel therapeutic options for autoimmune hepatitis. *Lancet Gastroenterol Hepatol*. 2021;6(4):315–326. doi: [10.1016/S2468-1253\(20\)30328-9](https://doi.org/10.1016/S2468-1253(20)30328-9).
7. Renand A, Habes S, Mosnier JF, Aublé H, Judor J-P, Vince N, Hulin P, Nedellec S, Métairie S, Archambeaud I. Immune alterations in patients with type 1 autoimmune hepatitis persist upon standard immunosuppressive treatment. *Hepatol Commun*. 2018;2(8):968–981. doi: [10.1002/hep4.1202](https://doi.org/10.1002/hep4.1202).
8. DeFrances MC, Debelius DR, Cheng J, Kane LP. Inhibition of T-cell activation by PIK3IP1. *Eur J Immunol*. 2012;42(10):2754–2759. doi: [10.1002/eji.201141653](https://doi.org/10.1002/eji.201141653).
9. Tang R, Wei Y, Li Y, Chen W, Chen H, Wang Q, Yang F, Miao Q, Xiao X, Zhang H, et al. Gut microbial profile is altered in primary biliary cholangitis and partially restored after UDCA therapy. *Gut*. 2018;67(3):534–541. doi: [10.1136/gutjnl-2016-313332](https://doi.org/10.1136/gutjnl-2016-313332).
10. Wei Y, Li Y, Yan L, Sun C, Miao Q, Wang Q, Xiao X, Lian M, Li B, Chen Y, et al. Alterations of gut microbiome in autoimmune hepatitis. *Gut*. 2020;69(3):569–577. doi: [10.1136/gutjnl-2018-317836](https://doi.org/10.1136/gutjnl-2018-317836).
11. Wang R, Tang R, Li B, Ma X, Schnabl B, Tilg H. Gut microbiome, liver immunology, and liver diseases. *Cell Mol Immunol*. 2021;18(1):4–17. doi: [10.1038/s41423-020-00592-6](https://doi.org/10.1038/s41423-020-00592-6).

12. Tilg H, Adolph TE, Dudek M, Knolle P. Non-alcoholic fatty liver disease: the interplay between metabolism, microbes and immunity. *Nat Metab.* 2021;3(12):1596–1607. doi: [10.1038/s42255-021-00501-9](https://doi.org/10.1038/s42255-021-00501-9).
13. Liwinski T, Casar C, Ruehleemann MC, Bang C, Sebode M, Hohenester S, Denk G, Lieb W, Lohse AW, Franke A, et al. A disease-specific decline of the relative abundance of Bifidobacterium in patients with autoimmune hepatitis. *Aliment Pharmacol Ther.* 2020;51(12):1417–1428. doi: [10.1111/apt.15754](https://doi.org/10.1111/apt.15754).
14. Krautkramer KA, Fan J, Bäckhed F. Gut microbial metabolites as multi-kingdom intermediates. *Nat Rev microbiol.* 2021;19(2):77–94. doi: [10.1038/s41579-020-0438-4](https://doi.org/10.1038/s41579-020-0438-4).
15. Roager HM, Licht TR. Microbial tryptophan catabolites in health and disease. *Nat Commun.* 2018;9(1). doi: [10.1038/s41467-018-05470-4](https://doi.org/10.1038/s41467-018-05470-4).
16. Pandey SP, Bender MJ, McPherson AC, Phelps CM, Sanchez LM, Rana M, Hedden L, Sangani KA, Chen L, Shapira JH, et al. Tet2 deficiency drives liver microbiome dysbiosis triggering Tc1 cell autoimmune hepatitis. *Cell Host Microbe.* 2022;30(7):1003–1019.e10. doi: [10.1016/j.chom.2022.05.006](https://doi.org/10.1016/j.chom.2022.05.006).
17. Vuerich M, Harshe R, Frank LA, Mukherjee S, Gromova B, Csizmadia E, Nasser IAM, Ma Y, Bonder A, Patwardhan V, et al. Altered aryl-hydrocarbon-receptor signalling affects regulatory and effector cell immunity in autoimmune hepatitis. *J Hepatol.* 2021;74(1):48–57. doi: [10.1016/j.jhep.2020.06.044](https://doi.org/10.1016/j.jhep.2020.06.044).
18. Gao L, Zhang W, Zhang L, Gromova B, Chen G, Csizmadia E, Cagle C, Nastasio S, Ma Y, Bonder A, et al. Silencing of aryl hydrocarbon receptor repressor restrains Th17 cell immunity in autoimmune hepatitis. *J Autoimmun.* 2024;143:103162. doi: [10.1016/j.jaut.2023.103162](https://doi.org/10.1016/j.jaut.2023.103162).
19. He X, Zhu Z, Johnson C, Stoops J, Eaker AE, Bowen W, DeFrances MC. Pik3ip1, a negative regulator of PI3K, suppresses the development of hepatocellular carcinoma. *Cancer Res.* 2008;68(14):5591–5598. doi: [10.1158/0008-5472.CAN-08-0025](https://doi.org/10.1158/0008-5472.CAN-08-0025).
20. Uche UU, Piccirillo AR, Kataoka S, Grebinoski SJ, D’Cruz LM, Kane LP. Pik3ip1/Trip restricts activation of T cells through inhibition of PI3K/Akt. *J Exp Med.* 2018;215(12):3165–3179. doi: [10.1084/jem.20172018](https://doi.org/10.1084/jem.20172018).
21. Chen Y, Wang J, Wang X, Li X, Song J, Fang J, Liu X, Liu T, Wang D, Li Q, et al. Pik3ip1 is a negative immune regulator that inhibits antitumor T-cell immunity. *Clin Cancer Res.* 2019;25(20):6180–6194. doi: [10.1158/1078-0432.CCR-18-4134](https://doi.org/10.1158/1078-0432.CCR-18-4134).
22. Xie W, Fang J, Shan Z, Guo J, Liao Y, Zou Z, Wang J, Wen S, Yang L, Zhang Y, et al. Regulation of autoimmune disease progression by Pik3ip1 through metabolic reprogramming in T cells and therapeutic implications. *Sci Adv.* 2022;8(39):eabo4250. doi: [10.1126/sciadv.abo4250](https://doi.org/10.1126/sciadv.abo4250).
23. Hennes EM, Zeniya M, Czaja AJ, Parés A, Dalekos GN, Krawitt EL, Bittencourt PL, Porta G, Boberg KM, Hofer H, et al. Simplified criteria for the diagnosis of autoimmune hepatitis. *Hepatology.* 2008;48(1):169–176. doi: [10.1002/hep.22322](https://doi.org/10.1002/hep.22322).
24. Powell DN, Swimm A, Sonowal R, Bretin A, Gewirtz AT, Jones RM, Kalman D. Indoles from the commensal microbiota act via the AHR and IL-10 to tune the cellular composition of the colonic epithelium during aging. *Proc Natl Acad Sci U S A.* 2020;117(35):21519–21526. doi: [10.1073/pnas.2003004117](https://doi.org/10.1073/pnas.2003004117).
25. Fujimori S, Chu PS, Teratani T, Harada Y, Suzuki T, Amiya T, Taniki N, Kasuga R, Mikami Y, Koda Y, et al. IL-15-producing splenic B cells play pathogenic roles in the development of autoimmune hepatitis. *JHEP Rep.* 2023;5(7):100757. doi: [10.1016/j.jhepr.2023.100757](https://doi.org/10.1016/j.jhepr.2023.100757).
26. Quintana FJ, Basso AS, Iglesias AH, Korn T, Farez MF, Bettelli E, Caccamo M, Oukka M, Weiner HL. Control of T(reg) and T(H)17 cell differentiation by the aryl hydrocarbon receptor. *Nature.* 2008;453(7191):65–71. doi: [10.1038/nature06880](https://doi.org/10.1038/nature06880).
27. Murter B, Kane LP. Control of T lymphocyte fate decisions by PI3K signaling. *F1000Res.* 2020;9:1171. doi: [10.12688/f1000research.26928.1](https://doi.org/10.12688/f1000research.26928.1).
28. Chapman NM, Boothby MR, Chi H. Metabolic coordination of T cell quiescence and activation. *Nat Rev Immunol.* 2020;20(1):55–70. doi: [10.1038/s41577-019-0203-y](https://doi.org/10.1038/s41577-019-0203-y).
29. Saravia J, Raynor JL, Chapman NM, Lim SA, Chi H. Signaling networks in immunometabolism. *Cell Res.* 2020;30(4):328–342. doi: [10.1038/s41422-020-0301-1](https://doi.org/10.1038/s41422-020-0301-1).
30. Shinde R, McGaha TL. The aryl hydrocarbon receptor: connecting immunity to the microenvironment. *Trends Immunol.* 2018;39(12):1005–1020. doi: [10.1016/j.it.2018.10.010](https://doi.org/10.1016/j.it.2018.10.010).
31. Rothhammer V, Quintana FJ. The aryl hydrocarbon receptor: an environmental sensor integrating immune responses in health and disease. *Nat Rev Immunol.* 2019;19(3):184–197. doi: [10.1038/s41577-019-0125-8](https://doi.org/10.1038/s41577-019-0125-8).
32. Stockinger B, Di Meglio P, Gialitakis M, Duarte JH. The aryl hydrocarbon receptor: multitasking in the immune system. *Annu Rev Immunol.* 2014;32(1):403–432. doi: [10.1146/annurev-immunol-032713-120245](https://doi.org/10.1146/annurev-immunol-032713-120245).
33. Zelante T, Iannitti RG, Cunha C, De Luca A, Giovannini G, Pieraccini G, Zecchi R, D’Angelo C, Massi-Benedetti C, Fallarino F, et al. Tryptophan catabolites from microbiota engage aryl hydrocarbon receptor and balance mucosal reactivity via interleukin-22. *Immunity.* 2013;39(2):372–385. doi: [10.1016/j.immuni.2013.08.003](https://doi.org/10.1016/j.immuni.2013.08.003).
34. Cervantes-Barragan L, Chai JN, Tianero MD, Di Luccia B, Ahern PP, Merriman J, Cortez VS, Caparon MG, Donia MS, Gilfillan S, et al. Lactobacillus reuteri induces gut intraepithelial CD4(+)CD8α(+) T cells. *Science.* 2017;357(6353):806–810. doi: [10.1126/science.aah5825](https://doi.org/10.1126/science.aah5825).
35. Liu Q, Li B, Li Y, Wei Y, Huang B, Liang J, You Z, Li Y, Qian Q, Wang R, et al. Altered faecal microbiome and metabolome in IgG4-related sclerosing cholangitis and primary sclerosing cholangitis. *Gut.* 2021;71(5):899–909. doi: [10.1136/gutjnl-2020-323565](https://doi.org/10.1136/gutjnl-2020-323565).

36. Postler TS, Ghosh S. Understanding the holobiont: how microbial metabolites affect human health and shape the immune system. *Cell Metab.* 2017;26(1):110–130. doi: [10.1016/j.cmet.2017.05.008](https://doi.org/10.1016/j.cmet.2017.05.008).
37. Swimm A, Giver CR, DeFilipp Z, Rangaraju S, Sharma A, Ulezko Antonova A, Sonowal R, Capaldo C, Powell D, Qayed M, et al. Indoles derived from intestinal microbiota act via type I interferon signaling to limit graft-versus-host disease. *Blood.* 2018;132(23):2506–2519. doi: [10.1182/blood-2018-03-838193](https://doi.org/10.1182/blood-2018-03-838193).
38. Wrzosek L, Ciocan D, Hugot C, Spatz M, Dupeux M, Houron C, Lievin-Le Moal V, Puchois V, Ferrere G, Trainel N, et al. Microbiota tryptophan metabolism induces aryl hydrocarbon receptor activation and improves alcohol-induced liver injury. *Gut.* 2020;70(7):1299–1308. doi: [10.1136/gutjnl-2020-321565](https://doi.org/10.1136/gutjnl-2020-321565).
39. Natividad JM, Agus A, Planchais J, Lamas B, Jarry AC, Martin R, Michel M-L, Chong-Nguyen C, Roussel R, Straube M, et al. Impaired aryl hydrocarbon receptor ligand production by the gut microbiota is a key factor in metabolic syndrome. *Cell Metab.* 2018;28(5):737–749.e734. doi: [10.1016/j.cmet.2018.07.001](https://doi.org/10.1016/j.cmet.2018.07.001).
40. Bender MJ, McPherson AC, Phelps CM, Pandey SP, Laughlin CR, Shapira JH, Medina Sanchez L, Rana M, Richie TG, Mims TS, et al. Dietary tryptophan metabolite released by intratumoral lactobacillus reuteri facilitates immune checkpoint inhibitor treatment. *Cell.* 2023;186(9):1846–1862.e1826. doi: [10.1016/j.cell.2023.03.011](https://doi.org/10.1016/j.cell.2023.03.011).
41. Duscha A, Gisevius B, Hirschberg S, Yissachar N, Stangl GI, Dawin E, Bader V, Haase S, Kaisler J, David C, et al. Propionic acid shapes the multiple sclerosis disease course by an immunomodulatory mechanism. *Cell.* 2020;180(6):1067–1080.e1016. doi: [10.1016/j.cell.2020.02.035](https://doi.org/10.1016/j.cell.2020.02.035).
42. Ehrlich AK, Pennington JM, Bisson WH, Kolluri SK, Kerkvliet NI. Tcdd, ficz, and other high affinity AhR ligands dose-dependently determine the fate of CD4+ T cell differentiation. *Toxicol Sci.* 2018;161(2):310–320. doi: [10.1093/toxsci/kfx215](https://doi.org/10.1093/toxsci/kfx215).
43. Bovensiepen CS, Schakat M, Sebode M, Zenouzi R, Hartl J, Peiseler M, Li J, Henze L, Woestemeier A, Schramm C, et al. Tnf-producing th1 cells are selectively expanded in liver infiltrates of patients with autoimmune hepatitis. *J Immunol.* 2019;203(12):3148–3156. doi: [10.4049/jimmunol.1900124](https://doi.org/10.4049/jimmunol.1900124).
44. Löhr HF, Schlaak JF, Lohse AW, Böcher WO, Arenz M, Gerken G, Meyer Zum Büschenfelde KH. Autoreactive CD4+ LKM-specific and anticolonotypic T-cell responses in LKM-1 antibody-positive autoimmune hepatitis. *Hepatology.* 1996;24(6):1416–1421. doi: [10.1053/jhep.1996.v24.pm0008938173](https://doi.org/10.1053/jhep.1996.v24.pm0008938173).
45. Rohlman D, Pham D, Yu Z, Stepan LB, Kerkvliet NI. Aryl hydrocarbon receptor-mediated perturbations in gene expression during early stages of CD4(+) T-cell differentiation. *Front Immunol.* 2012;3:223. doi: [10.3389/fimmu.2012.00223](https://doi.org/10.3389/fimmu.2012.00223).
46. Rosser EC, Piper CJM, Matei DE, Blair PA, Rendeiro AF, Orford M, Alber DG, Krausgruber T, Catalan D, Klein N, et al. Microbiota-derived metabolites suppress arthritis by amplifying aryl-hydrocarbon receptor activation in regulatory B cells. *Cell Metab.* 2020;31(4):837–851.e810. doi: [10.1016/j.cmet.2020.03.003](https://doi.org/10.1016/j.cmet.2020.03.003).
47. Chi H. Regulation and function of mTOR signalling in T cell fate decisions. *Nat Rev Immunol.* 2012;12(5):325–338. doi: [10.1038/nri3198](https://doi.org/10.1038/nri3198).